Inhibition of HDAC2 Protects the Retina From Ischemic Injury

Jie Fan,[1] Oday Alsarraf,[1] Mohammad Dahrouj,[1] Kenneth A. Platt,[2] C. James Chou,[3] Dennis S. Rice,[2] and Craig E. Crosson[1]

[1]Storm Eye Institute, Department of Ophthalmology, Medical University of South Carolina, Charleston, South Carolina
[2]Lexicon Pharmaceuticals, The Woodlands, Texas
[3]Departments of Pharmaceutical and Biomedical Sciences, Medical University of South Carolina, Charleston, South Carolina

Correspondence: Jie Fan, Department of Ophthalmology, 167 Ashley Avenue, Storm Eye Institute, Room 518, Medical University of South Carolina, Charleston, SC 29425; fan@musc.edu.

Submitted: December 19, 2012
Accepted: May 9, 2013

Citation: Fan J, Alsarraf O, Dahrouj M, et al. Inhibition of HDAC2 protects the retina from ischemic injury. *Invest Ophthalmol Vis Sci*. 2013;54:4072–4080. DOI:10.1167/iovs.12-11529

Purpose. Protein acetylation is an essential mechanism in regulating transcriptional and inflammatory events. Studies have shown that nonselective histone deacetylase (HDAC) inhibitors can protect the retina from ischemic injury in rats. However, the role of specific HDAC isoforms in retinal degenerative processes remains obscure. The purpose of this study was to investigate the role of HDAC2 isoform in a mouse model of ischemic retinal injury.

Methods. Localization of HDAC2 in mice retinas was evaluated by immunohistochemical analyses. To investigate whether selective reduction in HDAC2 activity can protect the retina from ischemic injury, *Hdac2*$^{+/-}$ mice were utilized. Electroretinographic (ERG) and morphometric analyses were used to assess retinal function and morphology.

Results. Our results demonstrated that HDAC2 is primarily localized in nuclei in inner nuclear and retinal ganglion cell layers, and HDAC2 activity accounted for approximately 35% of the total activities of HDAC1, 2, 3, and 6 in the retina. In wild-type mice, ERG a- and b-waves from ischemic eyes were significantly reduced when compared to pre-ischemia baseline values. Morphometric examination of these eyes revealed significant degeneration of inner retinal layers. In *Hdac2*$^{+/-}$ mice, ERG a- and b-waves from ischemic eyes were significantly greater than those measured in ischemic eyes from wild-type mice. Morphologic measurements demonstrated that *Hdac2*$^{+/-}$ mice exhibit significantly less retinal degeneration than wild-type mice.

Conclusions. This study demonstrated that suppressing HDAC2 expression can effectively reduce ischemic retinal injury. Our results support the idea that the development of selective HDAC2 inhibitors may provide an efficacious treatment for ischemic retinal injury.

Keywords: HDAC2, ischemia, retinal degeneration, neuroprotection

Histone acetylation is an active process regulated by the actions of two large families of enzymes—histone acetyltransferases (HATs) and histone deacetylases (HDACs), which modulate the chromatin structure by adding and removing acetyl groups from lysine residues in protein, respectively. The balance between the actions of HATs and HDACs functions as a pivotal regulatory mechanism for gene expression and controls numerous developmental processes and disease states. Histones are not the only target for HDACs and HATs. There is a rapidly growing list of nonhistone substrates including transcription factor p53[1] and other proteins.[2–4] Therefore, protein acetylation regulates not only gene expression, but many cytosolic activities as well.

Studies have shown that the dysregulated acetylation is associated with cancer and inflammatory[5] and cardiovascular diseases.[6] HDAC inhibitors are now approved for the treatment of different types of cancers (reviewed in Refs. 7, 8). In addition, the administration of nonselective HDAC inhibitors can suppress neuronal loss in central nervous system (CNS) models of ischemic injury and stroke.[9–14] In the retina, studies from this laboratory have shown that administering a nonselective HDAC inhibitor can suppress TNF-α expression and protect the retina from ischemic injury in rats.[15] However, HDAC activity is necessary for normal retinal development[16] and mediates retinal ganglion cell differentiation.[17] Hence, questions have arisen regarding whether suppression of specific HDAC isoforms offers any therapeutic advantage over nonselective HDAC inhibitors.

Although 18 HDAC isoforms exist, the current study focuses on the role of HDAC2 in the development of ischemic retinal injury. HDAC2 belongs to the class I HDAC family, and has been shown to negatively modulate synaptic plasticity, spine information, and memory.[18] The activation and/or overexpression of HDAC2 has been associated with the loss of memory.[19] More recent studies have demonstrated that selective inhibitors for HDAC2 protect against neural cell death.[20] These findings provide evidence that elevated HDAC2 activity plays an important role in neuronal dysfunction and degeneration. However, the roles of HDAC2 have not been evaluated in the retina. The goal of this study was to investigate the role of HDAC2 in ischemic retinal injury. To accomplish this we utilized a retinal ischemic mouse model and compared the efficacy of genetically suppressing HDAC2 expression to the pharmacological inhibition of total HDAC activity in reducing ischemic retinal injury.

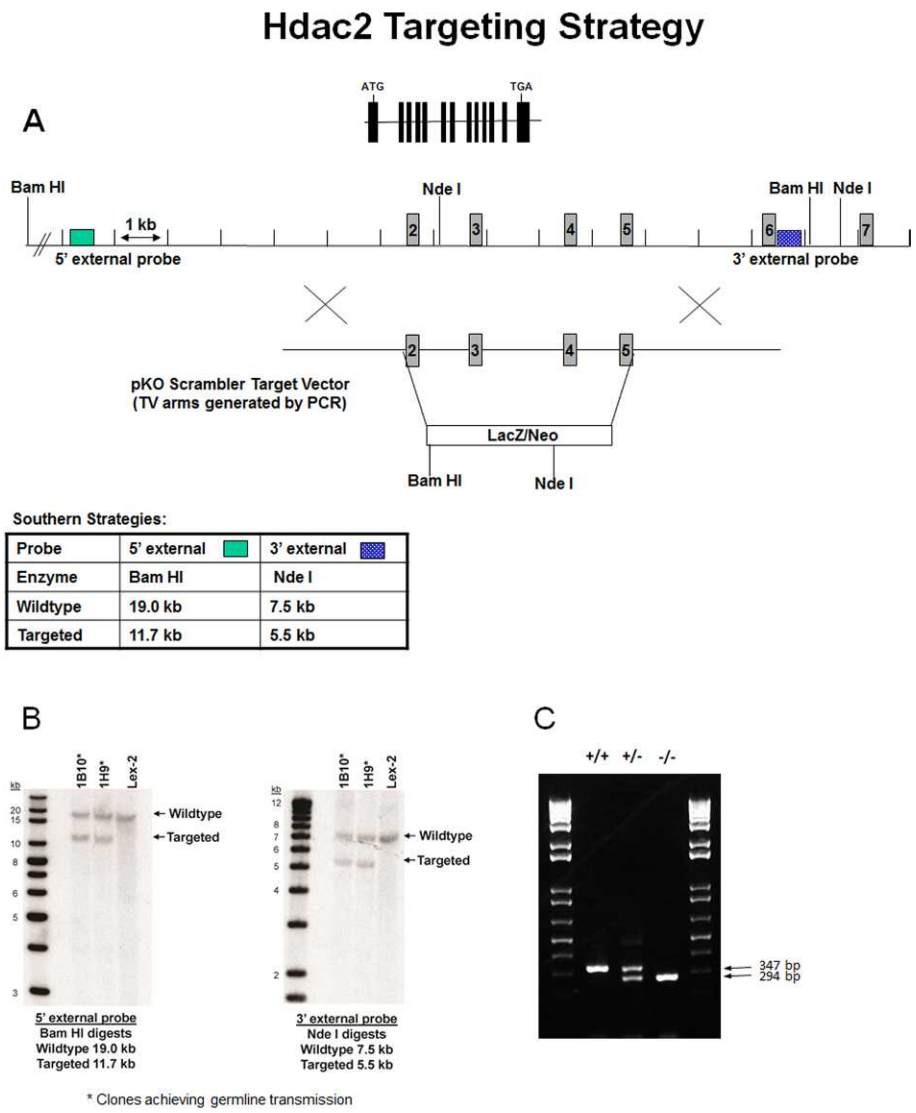

Figure 1. Targeted disruption of the *Hdac2* gene locus. (**A**) Targeting strategy used to disrupt the *Hdac2* locus. Homologous recombination (represented by X) between the targeting vector and the *Hdac2* gene results in the replacement of exons 2 to 5 with the selection cassette. (**B**) Southern hybridization indicating proper gene targeting in the embryonic stem cell clones. Clones 1B10 and 1H9 were selected for blastocyst injections; Lex2 represents untransfected embryonic stem cell DNA. (**C**) *Hdac2* genotyping results from $Hdac2^{+/+}$, $Hdac2^{+/-}$, and $Hdac2^{-/-}$ mice. DNA extract from mouse tails was amplified with PCR and KAPA2G Fast HotStart Genotyping Mix. The result indicates the deletion of *Hdac2* in $Hdac2^{-/-}$ mice.

Materials and Methods

Animals

Generation of Mutant HDAC2 Mice. The *Hdac2* mutant mice were generated by homologous recombination in embryonic stem (ES) cells where exons 2 to 5 of the *Hdac2* gene encoding a portion of the histone deacetylase domain were deleted (Fig. 1A). The *Hdac2* targeting vector was derived using long-range PCR to generate the 5′ and 3′ arms of homology using 129S5 ES cell DNA as a template. The 2536 bp 5′ arm was generated using primers *Hdac2*-3 [5′-ATGGATCC TATGACAGAAGTTTGTCGAAAGCTG-3′] and *Hdac2*-SfiA [5′-ATGGCCGCTATGGCCTGAGGCTTCATGGGATGACCCTGG-3′] and cloned using the TOPO (Invitrogen, Grand Island, NY) cloning kit. The 2718 bp 3′ arm was generated using primers *Hdac2*-SfiB [5′-ATGGCCAGCGAGGCCCCTGCAGAAGTGTGA GAAATAGACC-3′] and *Hdac2*-6 [5′-ATGGTACCAGCAGCATT CAGTGGGTCCACATG-3′] and cloned using the TOPO cloning kit. The 5′ arm was excised from the holding plasmid using BamH-I and Sfi I. The 3′ arm was excised from the holding plasmid using Sfi I and Kpn I. The arms were ligated to a Sfi I prepared selection cassette containing a β-galactosidase-neomycin marker and inserted into a BamH-I/Kpn I cut pKO Scrambler vector (Stratagene, Santa Clara, CA) to complete the *Hdac2* targeting vector, which results in the deletion of coding exons 2 to 5. The Not I linearized targeting vector was electroporated into 129S5 ES cells (Lex2). G418/FIAU-resistant ES cell clones were isolated, and correctly targeted clones were identified and confirmed by Southern blot analysis using a 297 bp 5′ external probe (14/15), generated by PCR using primers *Hdac2*-14 [5′-CACCCTAACACCATTACATTG-3′] and *Hdac2*-15 [5′-ACAACACATTCCAAGGACTTG-3′] and a 262 bp 3′ external probe (12/13), amplified by PCR using primers *Hdac2*-12 [5′-GCATAGGTTGTCTTGGGTAG-3′] and *Hdac2*-13 [5′-TCCTCA GAGCTTCTACATCC-3′]. Southern blot analysis using probe 14/15 detected a 19.0 Kb wild-type band and 11.7 Kb mutant band in BamH-I-digested genomic DNA, while probe 12/13

detected a 7.5 Kb wild-type band and 5.5 Kb mutants in Nde I-digested genomic DNA. Correctly targeted clones (Fig. 1B) were used to generate heterozygous mutant mice. Two targeted ES cell clones were identified and microinjected into C57BL/6 (albino) blastocysts to generate chimeric animals, which were bred to C57BL/6 (albino) females, and the resulting heterozygous offspring were interbred to produce homozygous *Hdac2*-deficient mice. Determination of the genotype of mice at the *Hdac2* locus was performed by extracting and screening DNA from tail biopsy samples using quantitative PCR and KAPA2G Fast HotStart Genotyping Mix (KaPa Biosystems, Inc., Woburn, MA) for the *Neo* cassette (Fig. 1C). This strategy enabled discrimination of zero, one, or two gene disruptions representing $Hdac2^{+/+}$, $Hdac2^{+/-}$, and $Hdac2^{-/-}$ mice, respectively. Age-matched wild-type littermates were used as control. We found that most of the *Hdac2*-null mice could not survive long enough for most of our experiments. This is consistent with another study reporting that *Hdac2*-null mice died early after birth due to severe cardiac malformations.[21] Therefore, *Hdac2* heterozygous knockout mice were used in the majority of the current studies. Animals were reared under cyclic light (12 hours light/12 hours dark) with ambient light intensity. Mice aged 10 to 12 weeks were used for experiments.

Trichostatin A (TSA) Treatment. To compare the effect of selective HDAC2 with general HDAC inhibition, $Hdac2^{+/+}$ mice were treated with the nonselective HDAC inhibitor, TSA. In these experiments, TSA (2.5 mg/kg) was injected intraperitoneally twice daily on days 0, 1, 2, and 3. Vehicle-treated mice were injected only with dimethyl sulfoxide on the same schedule. Mice were reared under cyclic light (12 hours light/12 hours dark) with the ambient light intensity; and at the time of the study, mice were 10 to 12 weeks old. All experiments were performed in accordance with the ARVO Statement for the Use of Animals in Ophthalmic and Vision Research; and the study protocol was approved by the Animal Care and Use Committee at the Medical University of South Carolina.

Retinal Ischemia

Retinal ischemia was induced using techniques described previously[22] with minor modifications. Mice were anesthetized with 300 mg/kg 1.25% Avertin solution (1.25 g 2,2,2-tribromoethanol, 2.5 mL tertiary-amyl alcohol in 100 mL phosphate-buffered saline [PBS]). Proparacaine (5 μL, 0.5%; Akorn, Inc., Buffalo Grove, IL) was applied for cornea analgesia. Body temperature was maintained on a heat pad at 37°C during the experiment. The anterior chamber was cannulated with a 33-gauge needle that was connected to a reservoir of sterile PBS, pH 7.4. The container was elevated to raise the intraocular pressure (IOP) to 120 mm Hg for 45 minutes. The IOP was monitored by a transducer connected to a computer. The contralateral eye was left untreated as a control.

Electroretinogram

Mice were dark adapted overnight and were anesthetized using xylazine (20 mg/kg, intraperitoneally) and ketamine (80 mg/kg, intraperitoneally). Pupils were dilated with phenylephrine hydrochloride (2.5%) and atropine sulfate (1%). Contact lens electrodes were placed on both eyes, accompanied by 2.5% Gonak hypromellose ophthalmic demulcent solution (Akorn, Lake Forest, IL). Full-field electroretinograms (ERGs) were recorded as described previously,[23] using the universal testing and electrophysiologic system 2000 (UTAS-2000; LKC Technologies, Gaithersburg, MD). Single flashes (10 ms) with intensity of 2.48 cd·s/m^2 were used for stimulation under scotopic conditions.

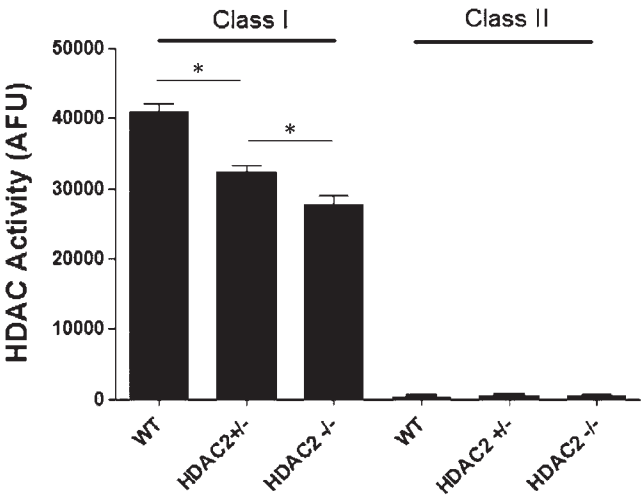

Figure 2. Class I and class II HDAC activities in $Hdac2^{+/+}$ ($n = 5$), $Hdac2^{+/-}$ ($n = 5$), and $Hdac2^{-/-}$ ($n = 3$) mouse retinas. Data are expressed as mean ± SE. *Indicates significant difference ($P < 0.05$).

Histology

For morphometric analyses, mouse eyes were enucleated and fixed in freshly made 4% paraformaldehyde in 0.1 M PBS for 2 hours at 4°C. After fixation, the tissues were dehydrated and embedded in paraffin. Retinal cross sections (5 μm thick) were then cut and stained with hematoxylin and eosin (Sigma-Aldrich, St. Louis, MO). Retinal sections were photographed and measured approximately 2 to 3 disc diameters from the optic nerve, using an Axioplan II microscope (Carl Zeiss, Inc., München-Hallbergmoos, Germany) and a ×20 objective lens. The number of cells in the retinal ganglion cell layer was determined by cell counts over a distance scale of 200 μm.

Immunohistochemistry

Eyes were enucleated and dissected, then fixed in freshly prepared 4% paraformaldehyde for 2 hours on ice. The eyes were washed three times with PBS and transferred into 15% sucrose in PBS and equilibrated for 1 hour on ice, followed by overnight incubation at 4°C in 30% sucrose in PBS. Tissues were embedded in optimal cutting temperature (OCT) compound (Tissue Tek; Sakura Finetech, Torrance, CA) and sectioned (12 μm thick) at −26°C. The sections were washed with PBS to remove OCT, and blocked with PBS containing 5% normal goat serum, 3% bovine serum albumin, and 0.1% Triton X-100 for 1 hour at room temperature. Acetyl histone-H3 and HDAC2 proteins were visualized by staining with primary polyclonal antibodies (Cell Signaling Technology, Beverly, MA, and Sigma-Aldrich, respectively) at a 1:500 dilution overnight at 4°C. The sections were washed three times with PBS for 15 minutes and incubated with Alexa Fluor 488 goat anti-rabbit secondary antibody (Invitrogen) at a 1:500 dilution for 2 hours at room temperature. Nuclei were stained with propidium iodide at 1:1000 (Sigma-Aldrich). Negative control was incubated only with Alexa Fluor 488 goat anti-rabbit secondary antibody and propidium iodide. Sections were imaged by means of a Leica confocal microscope (Leica, Wetzlar, Germany).

Investigative Ophthalmology & Visual Science

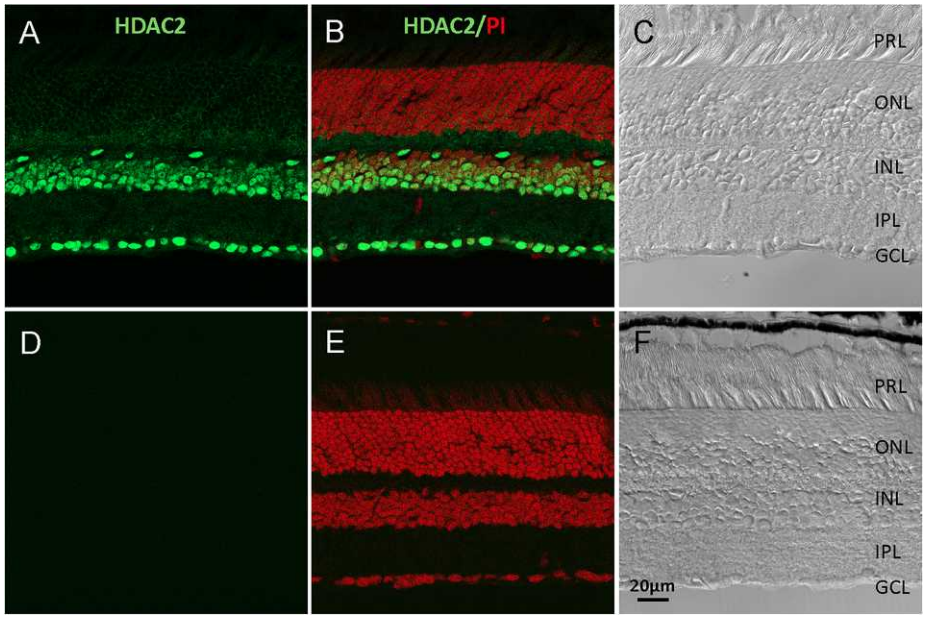

Figure 3. Localization of HDAC2 in mouse retina. (**A**) Immunohistochemical staining of HDAC2 (*green*). (**B**) Overlay of image A with propidium iodide, nuclei staining (*red*). (**C**) Bright-field image of (**A**). (**D**) Negative control, section was stained only with Alexa Fluor 488 anti-rabbit secondary antibody. (**E**) Overlay of image D with propidium iodide, nuclei staining (*red*). (**F**) Bright-field image of (**D**). PRL, photoreceptor layer; ONL, outer nuclear layer; INL, inner nuclear layer; IPL, inner plexiform layer; GCL, ganglion cell layer. *Scale bar*: 20 μm.

HDAC Activity Assay

The deacetylase activities of class I and class II were measured by assaying enzyme activity using the peptidase, trypsin, and the fluorophore-conjugated synthetic substrate, t-butoxyacetyl-lysine aminomethoxy-cumarin (Boc-Lys(Ac)-AMC) as previously described.[24] Briefly, lysates were diluted to a concentration of 1.0 μg/μL using standard HDAC buffer (50 mM Tris-Cl pH 8.0, 137 mM NaCl, 2.7 mM KCl, 1 mM $MgCl_2$, and 0.1 mg/mL bovine serum albumin) and incubated with the conjugated fluorophore acetylated lysine substrate Boc-Lys(Ac)-AMC in 96-well nonbinding plates (Greiner Bio-One, Monroe, NC) at room temperature for 2 hours. Baseline fluorescence was measured followed by treatment with the peptidase enzyme trypsin, freeing the fluorogenic 4-methylcoumarin-7-amide (AMC). The amount of fluorogenic AMC generated was then measured

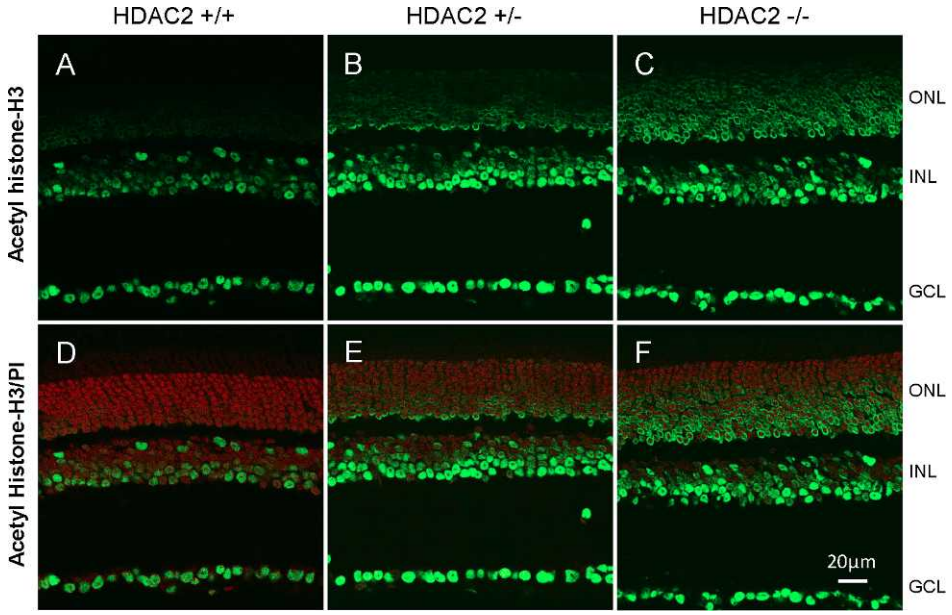

Figure 4. Acetylated histone-H3 immunostaining in mouse retina. Immunohistochemical staining of acetylated histone-H3 (*green*) in (**A**) *Hdac2*$^{+/+}$, (**B**) *Hdac2*$^{+/-}$, and (**C**) *Hdac2*$^{-/-}$ mouse retinas; and overlaid with propidium iodide, nuclei staining (*red*) in (**D**) HDAC2$^{+/+}$, (**E**) *Hdac2*$^{+/-}$, and (**F**) *Hdac2*$^{-/-}$ mouse retinas. ONL, outer nuclear layer; INL, inner nuclear layer; GCL, ganglion cell layer. *Scale bar*: 20 μm.

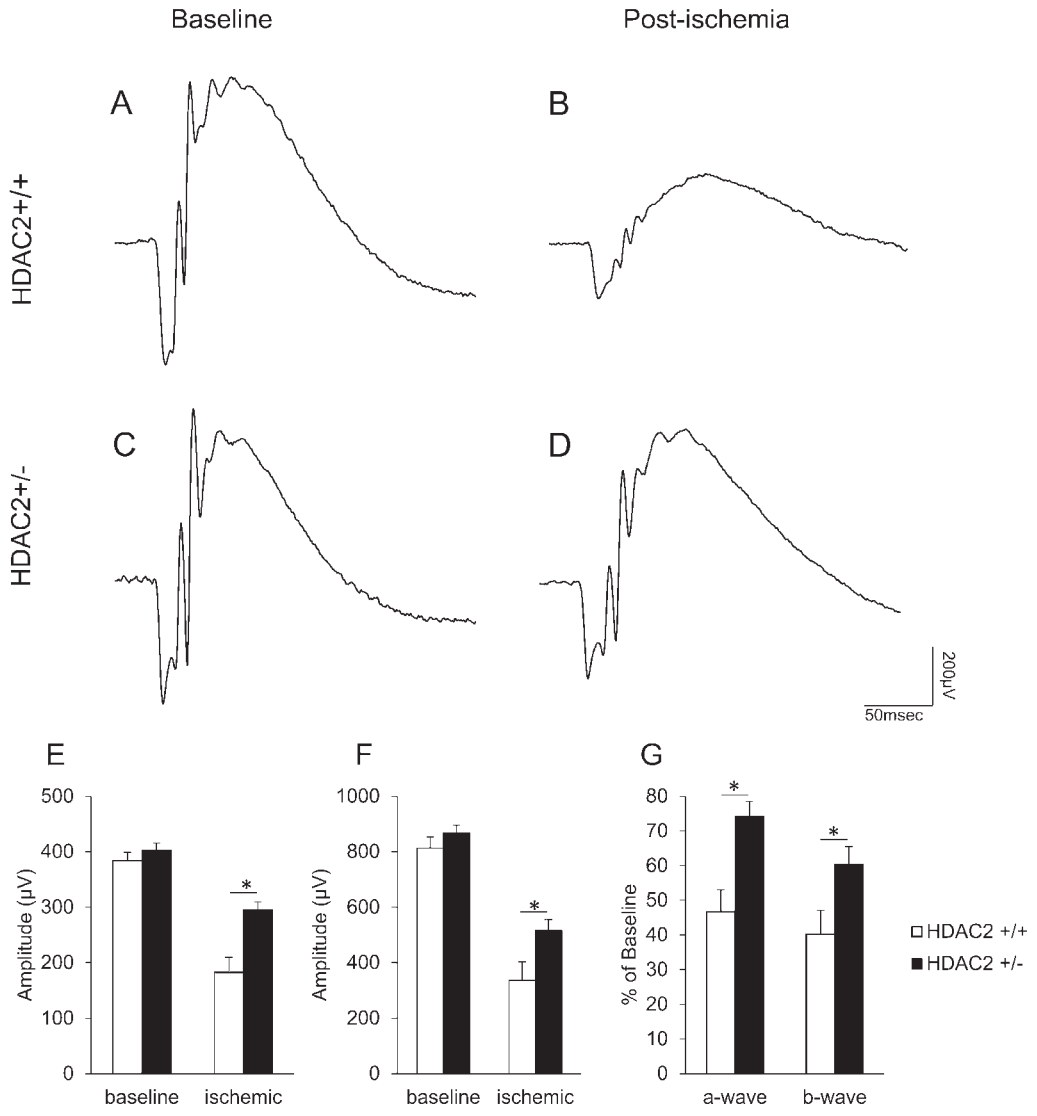

Figure 5. Effect of HDAC2 inhibition on electroretinogram responses. (**A**) Representative ERG before ischemic retinal injury in *Hdac2*$^{+/+}$ mouse. (**B**) Representative ERG recorded 7 days postischemia in *Hdac2*$^{+/+}$ mouse. (**C**) Representative ERG before ischemic retinal injury in *Hdac2*$^{+/-}$ mouse. (**D**) Representative ERG 7 days after ischemic retinal injury in *Hdac2*$^{+/-}$ mouse. Each ERG was obtained by averaging two responses to 2.48 cd·s/m^2 flashes with an interstimulus interval of 2 minutes. (**E**) Data analyses of ERG a-wave amplitudes before and 7 days after retinal ischemic injury. (**F**) Data analyses of ERG b-wave amplitudes before and 7 days after retinal ischemic injury. (**G**) Normalized a- and b-wave amplitudes 7 days after ischemic injury. Data are expressed as mean ± SE, $n = 10$. *Indicates significant difference ($P < 0.05$) between responses in *Hdac2*$^{+/+}$ and *Hdac2*$^{+/-}$ mice.

using an excitation wavelength of 355 nm and emission wavelength of 460 nm with a standard fluorospectrometer. The substrate for class I in this assay is specific to HDAC1, 2, 3, and 6.

Statistics

For all experiments, data were expressed as mean ± SE. Data were analyzed using a two-tailed Student's *t*-test, accepting a significance level of $P < 0.05$.

Results

Localization and Activity of HDAC2

Cross sections of retina from 3-month-old wild-type mice were probed with polyclonal HDAC2 antibody. We found that HDAC2 was primarily localized in the nuclei in inner nuclear and retinal ganglion cell layers (Fig. 2). No fluorescence staining was detected in the negative control.

The HDAC activity assays revealed that the total activities for HDAC1, 2, 3, and 6 in *Hdac2*$^{+/-}$ and *Hdac2*$^{-/-}$ retinas decreased 21.4 ± 2.3% and 35.1 ± 2.1% when compared to those of *Hdac2*$^{+/+}$ wild-type littermates (Fig. 3). The class II activities in retinas are negligible in all of these mice. To assess the functional consequences of suppressing HDAC2 expression, the level of retinal acetylated histone-H3 was evaluated in retina cross sections. In *Hdac2* wild-type retinas, acetylated histone-H3 was detected only in the inner nuclear and ganglion cell layers (Figs. 4A, 4D). In *Hdac2*$^{+/-}$ mice (Figs. 4B, 4E), immunolabeling of acetylated histone-H3 increased in the inner nuclear and ganglion cell layers and was also visible in the outer nuclear layer. In *Hdac2*$^{-/-}$ mice (Figs. 4C, 4F), heavy staining was observed in all retinal cell bodies. These results

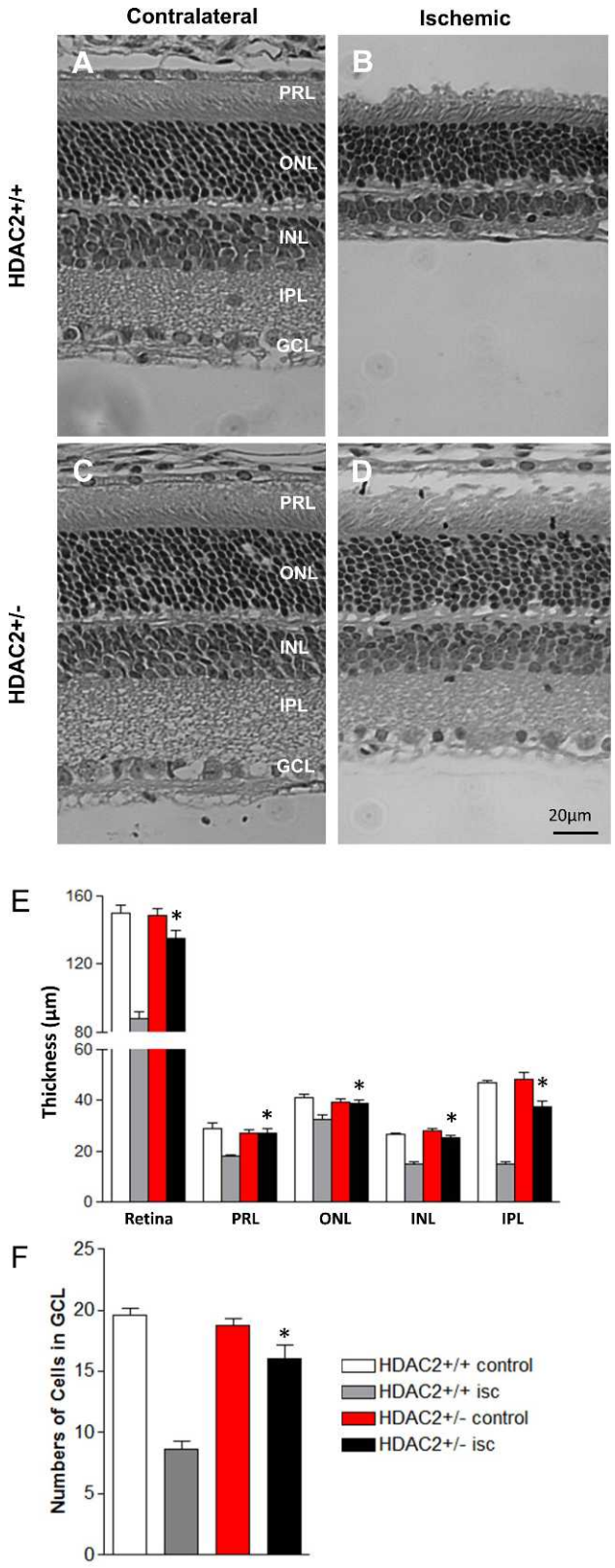

Figure 6. Effect of HDAC2 inhibition on retinal morphology before and 7 days after retinal ischemic injury. (**A**) Photomicrograph of retina cross section of contralateral eye in *Hdac2*$^{+/+}$ mouse. (**B**) Photomicrograph of retina cross section of ischemic eye in *Hdac2*$^{+/+}$ mouse. (**C**) Photomicrograph of retina cross section of contralateral eye in *Hdac2*$^{+/-}$ mouse. (**D**) Photomicrograph of retina cross section of ischemic eye from *Hdac2*$^{+/-}$ mouse. All images were taken 2 to 3 disc diameters from the optic nerve. *Scale bar*: 20 μm. (**E**) Data analyses of retinal layer thicknesses including total retina, photoreceptor (PR), outer nuclear layer (ONL), inner nuclear layer (INL), and inner plexiform layer (IPL). Data are presented as mean ± SE, $n = 6$. (**F**) Data analyses of cell body counts from retinal ganglion cell layer (GCL) over 200 μm distances. Data are presented as mean ± SE, $n = 6$. *Indicates significant difference ($P < 0.05$) between ischemic eyes in *Hdac2*$^{+/+}$ mice and *Hdac2*$^{+/-}$ mice.

are consistent with the loss of histone deacetylase activity in the *Hdac2*$^{+/-}$ and *Hdac2*$^{-/-}$ owing to the targeting strategy used to generate the mutant mice (Fig. 1A).

Effect of Reduced HDAC2 Expression on Ischemic Retinal Injury

To investigate the role of HDAC2 in the functional (scotopic ERG) and morphological changes resulting from ischemic retinal injury, we utilized *Hdac2* knockout mice. As most of the *Hdac2*$^{-/-}$ mice did not survive long enough for the experiments, *Hdac2*$^{+/-}$ mice were used in most experiments. In wild-type (*Hdac2*$^{+/+}$) mice, baseline a- and b-waves were 384.3 ± 14.4 and 812.9 ± 39.7 μV, respectively. In *Hdac2*$^{+/-}$ mice, baseline a- and b-waves were 402.4 ± 13.3 and 867.5 ± 27.8 μV, respectively. No significant differences in baseline ERG waveforms were noted between *Hdac2*$^{+/-}$ and *Hdac2*$^{+/+}$ mice. In wild-type mice 7 days following ischemic injury, ERG a- and b-waves were decreased by 53.3 ± 6.3% and 59.8 ± 6.9% of the baseline level in the ischemic eyes (Figs. 5A, 5B, 5G; white bars). No significant changes in waveform amplitudes were measured in the contralateral eye of these animals (Figs. 5A–C). In *Hdac2*$^{+/-}$ mice 7 days following ischemic injury, the ERG a- and b-waves were reduced by 25.8 ± 4.3% and 39.73 ± 5.2% of baseline levels, respectively (Figs. 5C, 5D, 5G; black bars). Although ERG waveforms were reduced in *Hdac2*$^{+/-}$ mice, these deficits were significantly less ($P < 0.05$) than those measured in the wild-type mice.

Figure 6 shows the changes in retinal morphology 7 days following unilateral retinal ischemia in wild-type and *Hdac2*$^{+/-}$ mice. In wild-type mice, total retinal thickness in the ipsilateral eye was decreased by 41.5 ± 2.4% when compared to the contralateral control eye. Although the photoreceptor layer and the outer nuclear layer exhibited mild thinning following ischemic injury, the majority of the retinal degenerations were found to be due to the loss of cell bodies in the inner nuclear layer and collapse of the inner plexiform layer (Figs. 6B, 6E). Ischemic injury also resulted in 56.1 ± 3.4% of cell loss from the retinal ganglion cell layer in wild-type mice (Fig. 6F; gray bar). However, in the *Hdac2*$^{+/-}$ mice, total retinal thickness following ischemic injury was significantly increased when compared to that in ischemic retinas from wild-type mice. In *Hdac2*$^{+/-}$ mice, no difference in the thickness of the photoreceptor and outer nuclear layers was measured, and only a slight reduction in the inner plexiform layer and inner nuclear layer thickness was measured (Fig. 6F; red and black bars). Finally, approximately 90% of the cells from the retinal ganglion cell layer remained in *Hdac2*$^{+/-}$ mice at 7 days postischemic injury (Fig. 6F; black bar).

Effect of Trichostatin A on Ischemic Retinal Injury

Trichostatin A is a general HDAC inhibitor, and this laboratory has shown that TSA administration can limit ischemic injury in Brown Norway rats.[15] In TSA-treated mice, baseline ERGs were similar to those recorded in *Hdac2*$^{+/-}$ and *Hdac2*$^{+/+}$ wild-type mice. In control, vehicle-treated mice, both a- and b-wave amplitudes were significantly decreased (48.5 ± 6.3% and 58.6

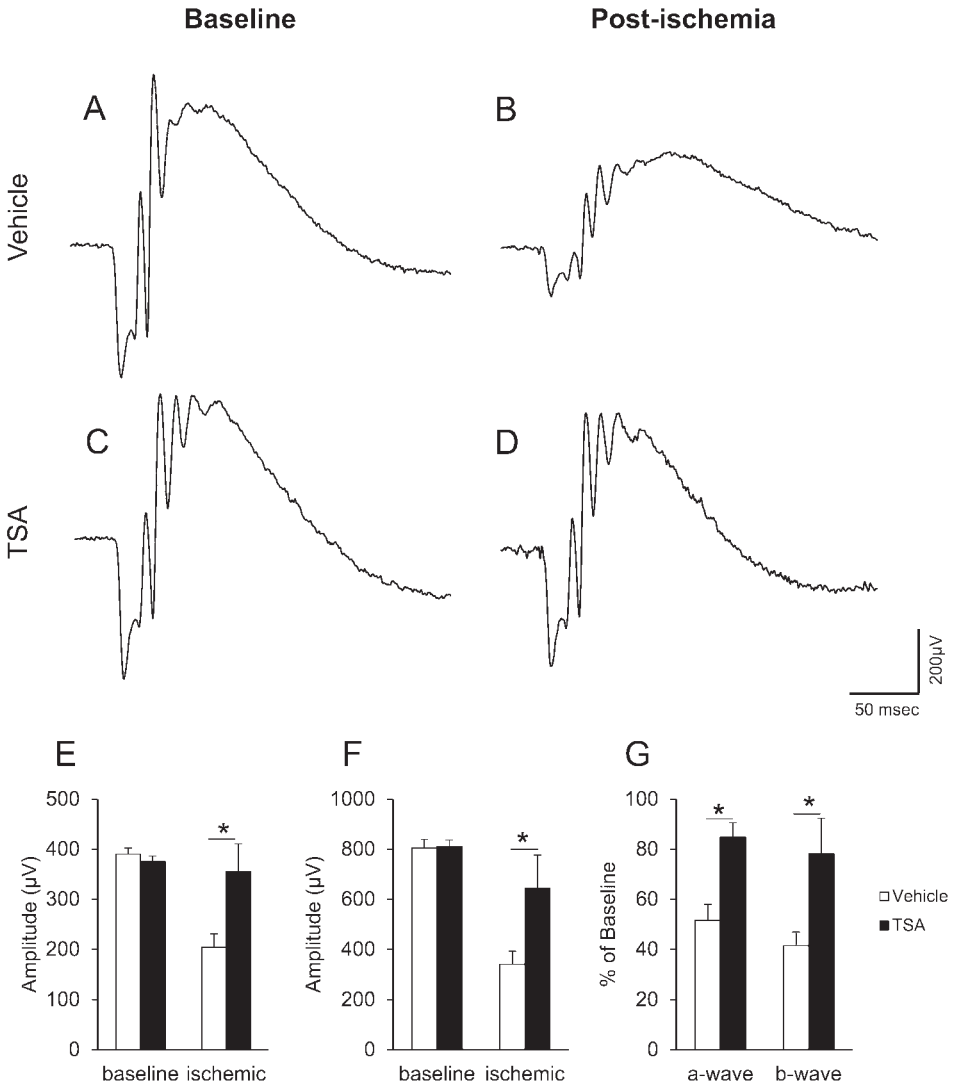

Figure 7. Effect of Trichostatin A (TSA; 2.5 mg/kg) on ERG responses. (**A**) Representative ERG before ischemic retinal injury in vehicle-treated *Hdac2*$^{+/+}$ mouse. (**B**) Representative ERG 7 days after ischemic retinal injury in vehicle-treated *Hdac2*$^{+/+}$ mouse. (**C**) Representative ERG before ischemic retinal injury in TSA-treated *Hdac2*$^{+/+}$ mouse. (**D**) Representative ERG 7 days after ischemic retinal injury in TSA-treated *Hdac2*$^{+/+}$ mouse. Animals were treated with vehicle or TSA (2.5 mg/kg) twice daily on days 0, 1, 2, and 3. Each ERG was obtained by averaging two responses to 2.48 cd·s/m^2 flashes with an interstimulus interval of 2 minutes. (**E**) Data analyses of ERG a-wave amplitudes before and 7 days after retinal ischemic injury. (**F**) Data analyses of ERG b-wave amplitudes before and 7 days after retinal ischemic injury. (**G**) Normalized a- and b-wave amplitudes 7 days after ischemic injury. Data are expressed as mean ± SE, $n \geq 3$. *Indicates significant difference ($P < 0.05$) between responses in the vehicle- and TSA-treated mice.

± 5.5% of baseline, respectively) following ischemic injury (Figs. 7A, 7B, 7G). In TSA-treated mice, the decrease of a- and b-wave amplitudes (15.2 ± 5.8% and 21.9 ± 14.2%) following ischemia was significantly less than that measured in vehicle-treated mice (Figs. 7C, 7D, 7G). In nonischemic eyes, administration of TSA did not produce any significant change in ERG responses (Figs. 7A, 7C). These data are consistent with the results obtained from rats.[15]

Discussion

Studies have shown that HDACs play important roles in acetylation homeostasis of histones and other proteins and in modulating transcription, cell cycle progression, differentiation, and apoptosis.[1,25,26] Imbalances in protein acetylation have become an emerging topic in the pathogenesis of cancer,[27] cardiovascular disease,[6] and neurodegenerative disorders.[28,29] In humans, 18 HDACs have been identified and are categorized into four classes depending on sequence identity and domain organization.[30] Inhibitors of class I and class II HDACs, now in clinical trial, show activity against several types of cancers (reviewed in Ref. 7) and represent novel therapeutic approaches to treat neurodegenerative and psychiatric disorders (reviewed in Ref. 31). Although studies in the brain have provided evidence that HDAC inhibitors are neuroprotective, their efficacy in ameliorating retina injuries is not well understood.

Initial studies in the murine retina demonstrated the expression of HDAC1, 3, 4, 5, and 6.[16,17] The activities of these isoforms are necessary for the development of several retinal neurons (rods, bipolar and ganglion cells) and Müller cells.[16,17] Subsequent studies provided evidence that HDAC4 plays an essential role in promoting the survival of retinal

neurons.[32] Studies have demonstrated that suppressing HDAC activity by TSA can protect the retina from ischemic injury in rats[15] and optic nerve crush.[33] HDAC inhibitors have been shown to suppress microglial activation and TNFα secretion[15,16] and to upregulate neuroprotective protein, such as heat shock protein.[34] In addition, HDAC inhibitors also limit the cellular response to the inflammatory cytokines by suppressing the activation of nuclear factor kappa-light-chain-enhancer of activated B cells and Janus kinase/signal transducer and activator of transcription and the secretion of metalloproteinases.[35–39] These discoveries have led us and others to conclude that HDACs play important roles in regulating retina development and the survival of retinal neurons following injury.

Although HDACs are ubiquitously expressed in all tissues, HDAC isoforms display distinct cellular locations. HDAC2 belongs to the class I HDAC family. Studies have shown that activation and overexpression of HDAC2 are associated with many cancers,[40–43] neurodegenerative diseases, and neural toxicity.[18] In amyotrophic lateral sclerosis patients, HDAC2 levels in the motor cortex and spinal cord are elevated.[44] Other studies have shown that HDAC2 negatively regulates synaptic plasticity, spine density, learning, and memory formation.[18] Loss of memory due to the activation and/or overexpression of HDAC2 has been restored by treatment with HDAC inhibitors like sodium valproate, sodium butyrate, and Vorinostat in an animal model of Alzheimer's disease.[19] More recent studies have demonstrated that moderately selective HDAC2 inhibitors can suppress neuronal cell death.[20] These findings support the idea that HDAC2 activity plays an important role in neurodegenerative diseases, and that HDAC2 may be a target for therapies in patients with neurodegenerative disorders.

In this study, we investigated the role of HDAC2 in ischemia-induced retinal degeneration and compared the effects of reducing HDAC2 activity genetically to the pharmacological effects of TSA, a nonselective HDAC inhibitor. As shown in Figure 3, the immune staining of HDAC2 was observed in the inner nuclear and ganglion cell layers. However, the increase in acetylated histone-H3 in the outer nuclear layer in the heterozygote and null mice indicated that HDAC2 is also expressed in photoreceptor cell bodies, albeit at lower levels. The activity measurements in *Hdac2*$^{-/-}$ mice revealed approximately 35% of the total activities for HDAC1, 2, 3, and 6. This suggested that the HDAC2 is a primary isoform in retinas. The fact that HDAC2 is localized primarily in the inner retinal layers, the same region where the majority of ischemic injury occurs (Fig. 6), suggested that selectively modulating the expression or activity of retinal HDAC2 may provide an efficacious therapy for reducing ischemic retinal injury.

To determine if selectively reducing HDAC2 expression can limit ischemic retinal injury, *Hdac2*$^{+/-}$ mice were subjected to a standard ischemic protocol, and compared to wild-type mice or mice treated with the nonselective HDAC inhibitor TSA. Results from this study demonstrated that ischemic retinal injury, as determined by morphometric and ERG analysis, was significantly reduced in *Hdac2*$^{+/-}$ mice when compared with wild-type control mice (Figs. 5, 6). To assess if the retinal neuroprotection afforded by reduced HDAC2 expression could be enhanced by more complete suppression of total HDAC activity, wild-type mice were treated with TSA (2.5 mg/kg) prior to and following ischemic injury. In mice receiving TSA, ERG responses revealed significantly larger a- and b-waves 7 days following ischemic injury when compared to mice that received vehicle treatment. While this neuroprotective response was similar to observations in previous studies using systemic administration of nonselective HDAC inhibitors in rats,[15] this improved functional response was slightly but not significantly greater than the neuroprotection afforded by reducing HDAC2 expression in *Hdac2*$^{+/-}$ mice. Whereas these data confirm the results from previous studies that HDAC activity is central to the development of inner retinal degeneration, based on the immunolocalization of HDAC2 and the neuroprotection afforded to *Hdac2*$^{+/-}$ mice, we conclude that the HDAC2 isoform is a vital isoform involved in mediating the degeneration associated with ischemic retinal injury.

In summary, results from this study demonstrate that HDAC2 expression is observed primarily in the inner retinal layers, but represents approximately 35% of the total activities of HDAC1, 2, 3, and 6 in the retina. Our results also provided the first evidence that the selective reduction in HDAC2 can significantly protect the retina from ischemic injury as measured by functional and morphometric analysis. Although multiple HDAC isoforms are expressed in the retina, HDAC2 appears to be the vital isoform involved in ischemic retinal degeneration. Hence, retinal HDAC2 appears to represent an attractive therapeutic target for the treatment of retinal ischemic disorders.

Acknowledgments

Supported by National Institutes of Health Grants EY021368 (CEC) and CA163452 (CJC), and an unrestricted grant to the Department of Ophthalmology at Medical University of South Carolina from Research to Prevent Blindness (RPB), New York, New York. The authors alone are responsible for the writing and content of the paper.

Disclosure: **J. Fan**, None; **O. Alsarraf**, None; **M. Dahrouj**, None; **K.A. Platt**, Lexicon Pharmaceuticals (E); **C.J. Chou**, None; **D.S. Rice**, Lexicon Pharmaceuticals (E); **C.E. Crosson**, None

References

1. Luo J, Su F, Chen D, Shiloh A, Gu W. Deacetylation of p53 modulates its effect on cell growth and apoptosis. *Nature*. 2000;408:377–381.
2. Kouzarides T. Acetylation: a regulatory modification to rival phosphorylation? *Embo J*. 2000;19:1176–1179.
3. Sterner DE, Berger SL. Acetylation of histones and transcription-related factors. *Microbiol Mol Biol Rev*. 2000;64:435–459.
4. Yang XJ. Lysine acetylation and the bromodomain: a new partnership for signaling. *Bioessays*. 2004;26:1076–1087.
5. Huang L. Targeting histone deacetylases for the treatment of cancer and inflammatory diseases. *J Cell Physiol*. 2006;209:611–616.
6. Zhang CL, McKinsey TA, Chang S, Antos CL, Hill JA, Olson EN. Class II histone deacetylases act as signal-responsive repressors of cardiac hypertrophy. *Cell*. 2002;110:479–488.
7. Tan J, Cang S, Ma Y, Petrillo RL, Liu D. Novel histone deacetylase inhibitors in clinical trials as anti-cancer agents. *J Hematol Oncol*. 2010;3:5.
8. Wagner JM, Hackanson B, Lubbert M, Jung M. Histone deacetylase (HDAC) inhibitors in recent clinical trials for cancer therapy. *Clin Epigenetics*. 2010;1:117–136.
9. Ferrante RJ, Kubilus JK, Lee J, et al. Histone deacetylase inhibition by sodium butyrate chemotherapy ameliorates the neurodegenerative phenotype in Huntington's disease mice. *J Neurosci*. 2003;23:9418–9427.
10. Gardian G, Browne SE, Choi DK, et al. Neuroprotective effects of phenylbutyrate in the N171-82Q transgenic mouse model of Huntington's disease. *J Biol Chem*. 2005;280:556–563.
11. Oliveira JM, Chen S, Almeida S, et al. Mitochondrial-dependent Ca2+ handling in Huntington's disease striatal cells: effect of histone deacetylase inhibitors. *J Neurosci*. 2006;26:11174–11186.

12. Petri S, Kiaei M, Kipiani K, et al. Additive neuroprotective effects of a histone deacetylase inhibitor and a catalytic antioxidant in a transgenic mouse model of amyotrophic lateral sclerosis. *Neurobiol Dis*. 2006;22:40–49.
13. Chang JG, Hsieh-Li HM, Jong YJ, Wang NM, Tsai CH, Li H. Treatment of spinal muscular atrophy by sodium butyrate. *Proc Natl Acad Sci U S A*. 2001;98:9808–9813.
14. Faraco G, Pancani T, Formentini L, et al. Pharmacological inhibition of histone deacetylases by suberoylanilide hydroxamic acid specifically alters gene expression and reduces ischemic injury in the mouse brain. *Mol Pharmacol*. 2006;70:1876–1884.
15. Crosson CE, Mani SK, Husain S, Alsarraf O, Menick DR. Inhibition of histone deacetylase protects the retina from ischemic injury. *Invest Ophthalmol Vis Sci*. 2010;51:3639–3645.
16. Chen B, Cepko CL. Requirement of histone deacetylase activity for the expression of critical photoreceptor genes. *BMC Dev Biol*. 2007;7:78.
17. Schwechter BR, Millet LE, Levin LA. Histone deacetylase inhibition-mediated differentiation of RGC-5 cells and interaction with survival. *Invest Ophthalmol Vis Sci*. 2007;48:2845–2857.
18. Guan JS, Haggarty SJ, Giacometti E, et al. HDAC2 negatively regulates memory formation and synaptic plasticity. *Nature*. 2009;459:55–60.
19. Kilgore M, Miller CA, Fass DM, et al. Inhibitors of class 1 histone deacetylases reverse contextual memory deficits in a mouse model of Alzheimer's disease. *Neuropsychopharmacol*. 2010;35:870–880.
20. Durham B. Novel histone deacetylase (HDAC) inhibitors with improved selectivity for HDAC2 and HDAC3 protect against neural cell death. *Biosci Horiz*. 2012;5:1–7.
21. Montgomery RL, Davis CA, Potthoff MJ, et al. Histone deacetylases 1 and 2 redundantly regulate cardiac morphogenesis, growth, and contractility. *Genes Dev*. 2007;21:1790–1802.
22. Husain S, Potter DE, Crosson CE. Opioid receptor-activation: retina protected from ischemic injury. *Invest Ophthalmol Vis Sci*. 2009;50:3853–3859.
23. Fan J, Rohrer B, Moiseyev G, Ma JX, Crouch RK. Isorhodopsin rather than rhodopsin mediates rod function in RPE65 knockout mice. *Proc Natl Acad Sci U S A*. 2003;100:13662–13667.
24. Wegener D, Wirsching F, Riester D, Schwienhorst A. A fluorogenic histone deacetylase assay well suited for high-throughput activity screening. *Chem Biol*. 2003;10:61–68.
25. Walkinshaw DR, Tahmasebi S, Bertos NR, Yang XJ. Histone deacetylases as transducers and targets of nuclear signaling. *J Cell Biochem*. 2008;104:1541–1552.
26. Wang C, Fu M, Mani S, Wadler S, Senderowicz AM, Pestell RG. Histone acetylation and the cell-cycle in cancer. *Front Biosci*. 2001;6:D610–D629.
27. Spiegel S, Milstien S, Grant S. Endogenous modulators and pharmacological inhibitors of histone deacetylases in cancer therapy. *Oncogene*. 2012;31:537–551.
28. Chuang DM, Leng Y, Marinova Z, Kim HJ, Chiu CT. Multiple roles of HDAC inhibition in neurodegenerative conditions. *Trends Neurosci*. 2009;32:591–601.
29. Saha RN, Pahan K. HATs and HDACs in neurodegeneration: a tale of disconcerted acetylation homeostasis. *Cell Death Differ*. 2006;13:539–550.
30. Dokmanovic M, Clarke C, Marks PA. Histone deacetylase inhibitors: overview and perspectives. *Mol Cancer Res*. 2007;5:981–989.
31. Abel T, Zukin RS. Epigenetic targets of HDAC inhibition in neurodegenerative and psychiatric disorders. *Curr Opin Pharmacol*. 2008;8:57–64.
32. Chen B, Cepko CL. HDAC4 regulates neuronal survival in normal and diseased retinas. *Science*. 2009;323:256–259.
33. Biermann J, Grieshaber P, Goebel U, et al. Valproic acid-mediated neuroprotection and regeneration in injured retinal ganglion cells. *Invest Ophthalmol Vis Sci*. 2010;51:526–534.
34. Ren M, Leng Y, Jeong M, Leeds PR, Chuang DM. Valproic acid reduces brain damage induced by transient focal cerebral ischemia in rats: potential roles of histone deacetylase inhibition and heat shock protein induction. *J Neurochem*. 2004;89:1358–1367.
35. Nasu Y, Nishida K, Miyazawa S, et al. Trichostatin A, a histone deacetylase inhibitor, suppresses synovial inflammation and subsequent cartilage destruction in a collagen antibody-induced arthritis mouse model. *Osteoarthritis Cartilage*. 2008;16:723–732.
36. Quivy V, Van Lint C. Regulation at multiple levels of NF-kappaB-mediated transactivation by protein acetylation. *Biochem Pharmacol*. 2004;68:1221–1229.
37. Wang X, Song Y, Jacobi JL, Tuan RS. Inhibition of histone deacetylases antagonized FGF2 and IL-1beta effects on MMP expression in human articular chondrocytes. *Growth Factors*. 2009;27:40–49.
38. Yang XJ, Gregoire S. Class II histone deacetylases: from sequence to function, regulation, and clinical implication. *Mol Cell Biol*. 2005;25:2873–2884.
39. Yuan ZL, Guan YJ, Chatterjee D, Chin YE. Stat3 dimerization regulated by reversible acetylation of a single lysine residue. *Science*. 2005;307:269–273.
40. Chang HH, Chiang CP, Hung HC, Lin CY, Deng YT, Kuo MY. Histone deacetylase 2 expression predicts poorer prognosis in oral cancer patients. *Oral Oncol*. 2009;45:610–614.
41. Fritzsche FR, Weichert W, Roske A, et al. Class I histone deacetylases 1, 2 and 3 are highly expressed in renal cell cancer. *BMC Cancer*. 2008;8:381.
42. Ropero S, Fraga MF, Ballestar E, et al. A truncating mutation of HDAC2 in human cancers confers resistance to histone deacetylase inhibition. *Nat Genet*. 2006;38:566–569.
43. Weichert W, Roske A, Gekeler V, et al. Histone deacetylases 1, 2 and 3 are highly expressed in prostate cancer and HDAC2 expression is associated with shorter PSA relapse time after radical prostatectomy. *Br J Cancer*. 2008;98:604–610.
44. Janssen C, Schmalbach S, Boeselt S, Sarlette A, Dengler R, Petri S. Differential histone deacetylase mRNA expression patterns in amyotrophic lateral sclerosis. *J Neuropathol Exp Neurol*. 2010;69:573–581.

Investigative Ophthalmology & Visual Science